Journal of Molecular Structure 1304 (2024) 137643

Contents lists available at ScienceDirect

Journal of Molecular Structure

journal homepage: www.elsevier.com/locate/molstr

Revisiting the vibrational spectrum of formic acid anhydride

Nanna Myllys [a,b,*], Irina Osadchuk [c], Jan Lundell [a]

[a] Department of Chemistry, University of Jyväskylä, P.O.Box 35, Jyväskylä, 40014, Finland
[b] Department of Chemistry, University of Helsinki, A.I. Virtasen aukio 1, Helsinki, 00014, Finland
[c] Department of Chemistry, Tallinn University of Technology, Acadeemia Tee 15, Tallinn, 12618, Estonia

ARTICLE INFO

Keywords:
Formic acid anhydride
Anharmonic calculations
Potential energy surface

ABSTRACT

The potential energy surface of formic acid anhydride has been investigated at highly accurate quantum chemical methods. The rotation of CHO group in global minimum conformer of formic acid anhydride can lead two different local minimum conformers. Both local minimum conformers are around three kcal/mol higher in energy than the global minimum conformer. One conformer is planar and another has two rotamers which rapidly interconvert to each others via planar transition state. In some earlier studies, this planar transition state has incorrectly assigned to be a local minimum structure. We calculated anharmonic vibrational frequencies for the global and local minimum energy conformers and compared the theoretical wavenumbers with experimental gas phase and argon matrix measurements. Our results suggest that some of the experimentally detected peaks are overtone and combination bands. In previous studies with harmonic calculations, those peaks have assigned to be fundamental bands with zero intensities. We confirmed that the higher energy conformer produced in argon matrix by ultra violet induced rotamerization of global minimum conformer belongs to the planar conformer.

1. Introduction

Formic acid anhydride (FAA) has been intensively investigated in the 1980s with experimental and computational methods [1–4]. Due to its characteristic strong absorption in the carbon stretching region, FAA has been the subject of many spectroscopical studies [5–8]. Later, FAA has also gained attention in the context of atmospheric and combustion chemistry [9–11]. For instance, FAA can form in the reaction of the smallest Criegee intermediate CH_2OO with formic acid, after the hydroperoxymethyl formate (HPMF) product decomposes [11–13]. While FAA has been established as the primary decomposition product of HPMF in the gas phase, it ultimately rearranges to formic acid and carbon monoxide through a unimolecular rearrangement mechanism [14]. Recently, Chung et al. studied molecular mechanisms of the reaction of CH_2OO with HCOOH by identifying different conformers of HMPF and FAA using infrared (IR) spectroscopy together with computational tools [8].

Already in the earliest spectroscopical studies of FAA, several peaks in the IR spectra were uncertain. For instance, electron diffraction study in 1972 indicated that the global minimum formic acid anhydride conformer is non-planar [15], but the theoretical and microwave investigations in 1975 firmly established a planar geometry of FAA structure [16,4]. The planar structure of lowest energy FAA has been confirmed in later spectroscopic and computational studies [1,5,17]. To accurately analyse the vibrational spectrum of FAA, an anharmonic computational treatment of vibrational frequencies is needed. The measured spectrum might contain overtone and combination bands, which are out of reach with harmonic calculations. In addition, all three rotational conformers of FAA need to be modeled to verify whether earlier interpretations about the structures and energetics, as well as the assignment of vibrational frequencies, remain valid when using anharmonic rather than harmonic frequencies, together with coupled cluster theory energy corrections. In addition of re-evaluating the structures, energies and vibrational spectra of all conformers of formic acid anhydride, we have computed the Raman scattering activities (and theoretical Raman intensities) to guide future experimental Raman spectroscopy studies.

2. Computational details

We have used three levels of theory to optimize structures and calculate vibrational frequencies: MP2/aug-cc-pVTZ for the most accurate energies and frequencies [18,19], B3LYP/aug-cc-pVTZ as it generally

* Corresponding author at: Department of Chemistry, University of Jyväskylä, P.O.Box 35, Jyväskylä, 40014, Finland.
E-mail address: nanna.myllys@helsinki.fi (N. Myllys).

https://doi.org/10.1016/j.molstruc.2024.137643
Received 24 November 2023; Received in revised form 15 January 2024; Accepted 25 January 2024
Available online 30 January 2024

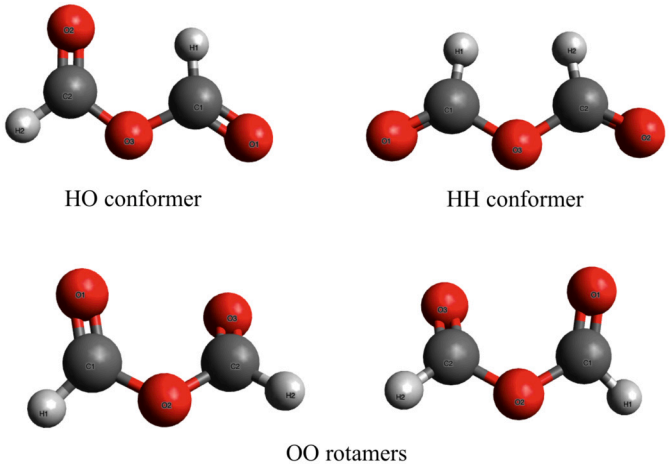

Fig. 1. Global (HO) and local (HH and OO) minimum structures of formic acid anhydride. The OO conformer has two rotamers which rapidly interconvert to each others.

leads good vibrational spectra [20–22] and B3LYP-D3/aug-cc-pVTZ to reach good accuracy with reasonable computational cost [23]. For a reliable comparison of theoretical and experimental vibrational spectra, anharmonic frequency calculations are performed using vibrational second order perturbation theory (VPT2) [24,25] with B3LYP, B3LYP-D3 and MP2 methods as implemented in Gaussian16 RevA.03 [26]. Raman scattering activities for fundamental bands are obtained using the B3LYP/aug-cc-pVTZ level. For a state-of-the-art energy description, highly correlated electronic energy corrections at the RI-CCSD(T)-F12/cc-pVTZ-F12 level of theory (as implemented in Orca v4.2.1) are performed on top of the B3LYP, B3LYP-D3 and MP2 structures [27–29]. Dipole moments are calculated at the RI-CCSD(T)-F12/cc-pVTZ-F12 level on top of the MP2/aug-cc-pVTZ structure (note, all levels gave similar dipole moments within 0.1 D).

3. Results and discussion

By using a set of quantum chemical calculations (discussed in detail later) we have found several meaningful stationary points for formic acid anhydride. Minimum energy structures include HO, HH and OO conformers of FAA and the OO conformer can further be divided into two rotamers which are each others mirror images (see Fig. 1). The global minimum HO conformer is a planar structure with a point group of C_s and a dipole moment of 1.8 D. The HH conformer has the highest symmetry and dipole moment (C_{2v} point group and 3.3 D dipole). The OO conformer belongs to the C_2 point group and has a dipole moment of 3.1 D.

It should be mentioned that in the literature, FAA conformers have several different naming styles: for instance, AE (HO), EE (HH) and AA (OO), where A is axial and E is equatorial (e.g. Lundell at al. [5,6]), [sp,ap] (HO), [ap,ap] (HH) and [sp,sp] (OO), where ap denotes antiplanar and sp synperiplanar (e.g. Wu et al. [7]) and *anti* (HO) and *syn* (OO) (e.g. Chung et al. [8]).

Fig. 2 shows the molecular structures of transition states connecting minimum energy configurations to each others. TS(HH) and TS(OO) belong to the C_1 point group and they have dipole moments of 3.0 and 2.7 D, respectively. TS(planarOO) has C_{2v} symmetry and a dipole moment of 3.3 D.

3.1. Potential energy surface of formic acid anhydride

In order to study the potential energy surface of FAA, we have performed a relaxed scan for the rotations of an axial and an equatorial CHO group. Fig. 3 shows the electronic energy relative to the global minimum structure for each point of a scan at three levels of theory.

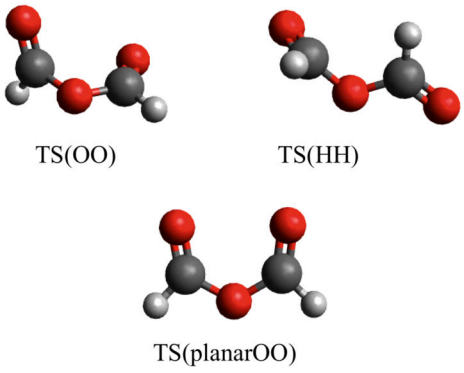

Fig. 2. Transition state structures connecting HO and HH conformers (TS(HH)), HO and OO conformers (TS(OO)) and OO rotamers (TS(planarOO)).

The rotation leading to the HH conformer has a barrier almost twice high as that leading to the OO conformer. At the MP2 level, the electronic energy barriers for forming the HH conformer (TS(HH)) and OO conformer (TS(OO)) are 8.43 kcal/mol and 4.37 kcal/mol, respectively. Thus it is clear that OO is the kinetic product of the FAA rotation from its minimum structure.

The HH conformer is a local minimum on the potential energy surface, which can be reached by rotating the axial CHO group of the HO conformer by 180 degrees. The electronic energy of the HH conformer is 2.82 kcal/mol above the global minimum at MP2 level. Rotation of the equatorial CHO group of a HO conformer by 180 degrees leads to a planar structure where both CHO groups are in axial positions. This is a transition state (TS(planar)), which connects two local minimum configurations, the OO rotamers, to each others. In the OO rotamers, both O=C-O-C dihedral angles are 22 degrees. These two rotamers are each others mirror images. They have identical energies and other properties, and rapidly interconvert over an electronic energy barrier of only 0.36 kcal/mol at the MP2 level. The electronic energy of the OO conformers is 2.62 kcal/mol above the global minimum at the MP2 level. This means that the OO conformer is slightly lower in electronic energy than HH conformer at the MP2 level. Qualitatively similar results can be obtained using the B3LYP-D3 functional. However, when using the density functional B3LYP without any dispersion corrections, the results differ even qualitatively, as B3LYP suggest the HH conformer to be lower in energy than the OO conformer. This energy order has been suggested also in earlier studies [1,5]. However, these studies did not find the actual local minimum OO conformer, and instead carried out calculations on the TS(planarOO) structure.

The electronic energies relative to the HO conformer (ΔE_{el}) are given in Table 1 at the B3LYP/aug-cc-pVTZ, B3LYP-D3/aug-cc-pVTZ and MP2/aug-cc-pVTZ levels (which correspond to energies shown in Fig. 3). In addition, ΔE_{el} values calculated at the RI-CCSD(T)-F12/cc-pVTZ-F12 on top of the B3LYP, B3LYP-D3 and MP2 structures are listed. Anharmonic zero-point corrected electronic energies (ΔE_0) at the same six level of theories are also given in Table 1. Both ΔE_{el} and ΔE_0 values using any other method than B3LYP suggest that the OO conformer is lower in energy than the other local minimum structure HH. Thus we can conclude that the OO conformer is the thermodynamic product of FAA rotation from the minimum-energy structure (HO). The qualitative failure of the B3LYP method is not surprising [30,31], and these results simply confirm once more that uncorrected B3LYP is not a suitable functional for calculating accurate energetics even for simple non-H-bonding system.

3.2. Vibrational spectra of formic acid anhydride

As the HO conformer is the global minimum energy structure, the majority of the experimental data measured for FAA corresponds to the HO conformer. The Gibbs free energy difference at 298 K be-

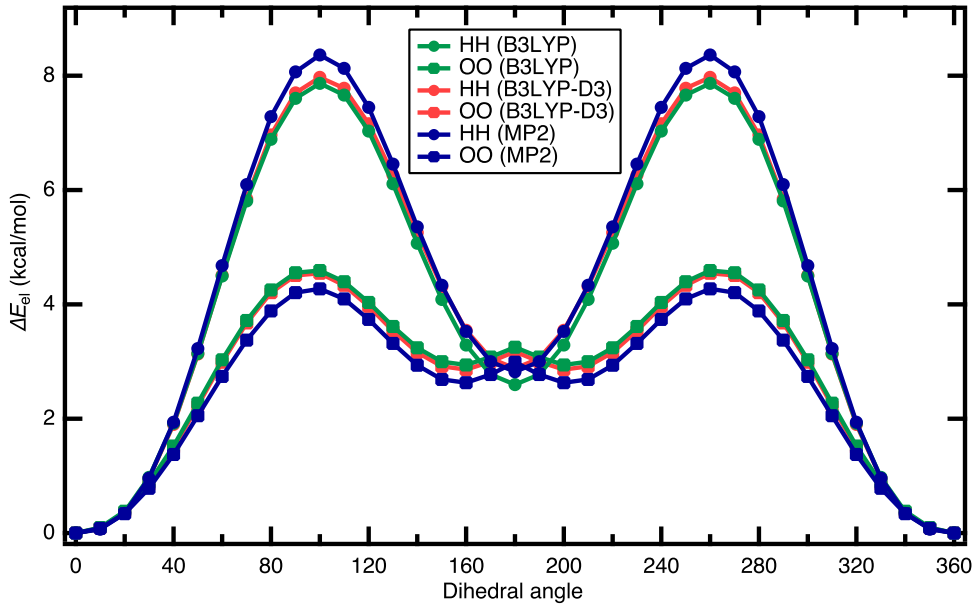

Fig. 3. Relative electronic energies of -CHO rotation as a function of torsion angle.

Table 1
Calculated electronic energies (ΔE_{el}) and zero-point corrected energies (ΔE_0) in kcal/mol relative to the global minimum energy HO conformer.

ΔE_{el}	HH	OO	TS(HH)	TS(OO)	TS(planarOO)
B3LYP	2.59	2.94	7.87	4.61	3.25
B3LYP-D3	2.88	2.85	7.98	4.56	3.17
MP2	2.82	2.62	8.36	4.28	2.98
CCSD(T)//B3LYP	3.17	2.89	8.49	4.48	3.27
CCSD(T)//B3LYP-D3	3.16	2.85	8.44	4.42	3.24
CCSD(T)//MP2	3.19	2.85	8.43	4.37	3.27
ΔE_0	HH	OO	TS(HH)	TS(OO)	TS(planarOO)
B3LYP	2.52	2.81	7.40	4.33	3.02
B3LYP-D3	2.77	2.73	7.50	4.28	2.95
MP2	2.73	2.51	7.88	4.03	2.76
CCSD(T)//B3LYP	3.10	2.76	8.02	4.20	3.04
CCSD(T)//B3LYP-D3	3.05	2.73	7.97	4.14	3.01
CCSD(T)//MP2	3.10	2.73	7.95	4.13	3.04

tween the HO conformer and the HH and OO conformers are 3.9 and 3.3 kcal/mol (at the RI-CCSD(T)-F12/cc-pVTZ-F12//MP2/aug-cc-pVTZ level), respectively. Thus the HO structure dominates the Boltzmann distribution even at room temperature, making HH and OO conformers difficult or even impossible to observe in the gas phase. However, matrix isolation techniques allow the detection of higher energy species. Indeed, another FAA conformer was produced by irradiating the global minimum structure by ultraviolet light in an argon matrix, and it was further characterized by infrared spectroscopy [5]. Thus, we compare our theoretical results to an experimental IR spectra measured in an Ar matrix. As B3LYP and B3LYP-D3 yield almost identical vibrational frequencies and B3LYP is commonly used method in theoretical vibrational spectroscopy, only B3LYP results are given here. Table 2 gives the calculated anharmonic transition energies and integrated intensities for fundamental and overtone bands as well as for the five highest intensity (at MP2 level) combination bands.

In previous studies where anharmonic calculations were infeasible, all of the experimental bands have been identified to be fundamental vibrations. The experimental wavenumber 1067 cm^{-1} has been assumed to be the $1\nu_8$ vibration as that was closest match with a calculated harmonic wavenumber. However, with current computational methods, we are able to calculate anharmonic wavenumbers and intensities for fundamental, overtone, and combination bands, which allows us to compare theoretical and experimental spectra more reliably. Indeed, while the fundamental vibration $1\nu_8$ has a wavenumber relatively close to the computed one (1035 cm^{-1} at the MP2 level), the integrated anharmonic intensity for that band is 0 km/mol. Thus it is more likely that the band actually corresponds an overtone vibration $2\nu_{12}$, for which the MP2 wavenumber and intensity are 1065 cm^{-1} and 10 km/mol, respectively.

The computed anharmonic intensities of some of the combination bands indicate that they could be visible in an experimental spectrum. The highest intensity combination band (at the MP2 level), $1\nu_6 + 1\nu_2$, has an intensity of almost 100 km/mol, which is the fourth highest intensity of the all peaks. However, the wavenumber of that combination band is very close to that of the high intensity $1\nu_7$ fundamental band, which makes it difficult to separate it from a spectrum. In a similar manner, the combination band $1\nu_9 + 1\nu_5$ has quite high intensity, but as the higher intensity $1\nu_4$ fundamental band has a wavenumber close to that of this combination band, they are difficult to identify as separate peaks. However, anharmonic approach also has limitations, for example in description of Fermi resonance. It has been discussed in previous studies [1,6] that an observed 1077 cm^{-1} absorption arises from a Fermi resonance between high intensity bands $1\nu_7$ and $1\nu_{10}$. The stretching modes between a central oxygen and carbon atoms are strongly coupled to the skeletal O–C–O bending mode. To further study this Fermi resonance, new laboratory measurements involving infrared pumping should be performed.

We have calculated the mean absolute errors (MAEs) for each level of theory based on the difference between calculated gas-phase wavenumbers and experimental argon matrix wavenumbers. The MAEs for B3LYP and MP2 are 18 and 8 cm^{-1}, respectively, which shows that B3LYP leads to decent agreement with experimental spectra, whereas MP2 performs even better and leads to very good agreement with experiments. However, it should keep in mind that MP2 is computationally more demanding than density functional theory (DFT), and anharmonic MP2 calculations are not applicable to systems much larger than an isolated FAA molecule. Thus, we have benchmarked anharmonic frequencies using B3LYP and B3LYP-D3 functionals with different basis sets (see Supporting Information). We found that a small Pople's basis set, 6-31+G(d), yields good accuracy with both functionals, with MAE for B3LYP 12 and for B3LYP-D3 14 cm^{-1}. Thus in studies of larger molecules, a suitable density functional with a 6-31+G(d) basis is recommended to obtain a good accuracy with a low computational cost.

Table 2
Experimental wavenumbers (ν in cm^{-1}) in the gas phase and in Ar matrix, calculated anharmonic ν wavenumbers using the B3LYP and MP2 methods for the HO conformer of FAA, differences between gas phase and calculated wavenumbers ($\Delta\nu$), calculated anharmonic intensities (I in km/mol) for fundamentals (1ν), overtones (2ν) and highest intensity combination bands ($1\nu + 1\nu$), and assignment of vibrations for fundamental bands.

	gas	Ar	B3LYP			MP2			assignment
	ν	ν	ν	I	$\Delta\nu$	ν	I	$\Delta\nu$	(see Fig. 1 for labeling)
$1\nu_1$	2987	2992	2941	17	46	3000	18	-13	H1-C1str.
$1\nu_2$	2967	2965	2912	29	55	2978	13	-11	H2-C2str.
$1\nu_3$	1812	1812	1836	105	-24	1804	77	8	O1=C1str.
$1\nu_4$	1762	1762	1774	454	-12	1747	382	15	O2=C2str.
$1\nu_5$	1381	1382	1375	2	6	1381	5	0	H2rock
$1\nu_6$	1359	1359	1356	1	3	1357	1	2	H1rock
$1\nu_7$	1090	1091	1071	512	19	1089	482	1	O3-C2str.
$1\nu_8$			1039	0		1035	0		C-Hwag.,asym.
$1\nu_9$			1006	0		1004	1		C-Hwag.,sym.
$1\nu_{10}$	998	998	974	271	24	983	261	15	O3-C1str.
$1\nu_{11}$	776	775	767	10	9	763	10	13	O2=C2-H2scissor
$1\nu_{12}$	540	540	535	5	5	533	4	7	O1=C1-H1scissor
$1\nu_{13}$	260		252	8	8	259	7	1	C1-O3-C2scissor
$1\nu_{14}$	227		226	14	1	218	13	9	H2twist
$1\nu_{15}$	85		116	24	-31	93	28	-8	H1twist
$2\nu_1$			5761	1		5893	1		
$2\nu_2$			5704	1		5861	1		
$2\nu_3$			3652	4		3575	4		
$2\nu_4$			3537	2		3487	2		
$2\nu_5$			2731	0		2746	0		
$2\nu_6$			2696	0		2699	0		
$2\nu_7$			2125	7		2159	6		
$2\nu_8$			2047	0		2048	0		
$2\nu_9$			2037	0		2024	0		
$2\nu_{10}$			1940	13		1954	10		
$2\nu_{11}$			1531	0		1524	0		
$2\nu_{12}$	1067		1068	22	-1	1065	10	2	
$2\nu_{13}$			504	0		518	0		
$2\nu_{14}$			450	0		433	0		
$2\nu_{15}$			261	3		206	2		
$\nu_6+\nu_2$			1151	6		1100	97		
$\nu_9+\nu_5$			1729	1		1732	26		
$\nu_6+\nu_1$			1147	1		1115	9		
$\nu_{11}+\nu_1$			2044	6		2068	7		
$\nu_{14}+\nu_8$			3597	4		3533	6		

Tables 3 and 4 list the calculated anharmonic transition energies and integrated intensities for the HH and OO conformers of FAA, respectively. We have compared the experimental vibrational spectra measured for a local minimum energy FAA conformer in an Ar matrix to our theoretical results for HH and OO conformers to assign the peaks and determine which conformer was actually detected. There are five experimental wavenumbers available, and we have assigned them to correspond the best match with a calculated wavenumber at each level of theory, and calculated the MAE. As Table 3 shows, four of the five experimental wavenumbers can be assigned to the same calculated wavenumber for all levels of theory, but the vibrational with a wavenumber of 1039 cm^{-1} could be either $1\nu_8$, as the MP2 method suggests, or $2\nu_{12}$ as the DFT results indicate. MAEs for each method based on the smallest $\Delta\nu$ values for B3LYP and MP2 are 17 and 7 cm^{-1}, respectively. As the calculated intensity for $1\nu_8$ is much higher than that of $2\nu_{12}$, and as the MP2 method is more accurate than DFT, it is likely that the 1039 cm^{-1} vibration corresponds $1\nu_8$. The recalculated MAE for B3LYP would then be 22 cm^{-1}. It should be noted that the computed intensity of the $1\nu_4$ vibration is quite high, but that peak does not appearing in any experimental spectrum. The wavenumber of this peak, 1780 cm^{-1}, is very close to the wavenumber of the $1\nu_4$ vibration of the HO conformer (1762 cm^{-1}). It is therefore possible that it has simply not been detected as a separate peak. The highest intensity combination band, $1\nu_{13} + 1\nu_4$, could also be visible, but as the fundamental band $1\nu_3$ is very close to it, peak separation is again difficult.

The same experimental wavenumbers for a local minimum are also compared with the calculated wavenumbers of the OO conformer in Table 4. There are two experimental bands for which the closest theoretical band depends on the method. Wavenumber 2932 cm^{-1} could be either the $1\nu_1$ or the $1\nu_2$ vibration, while wavenumber 1039 cm^{-1} can be assigned to either $1\nu_7$ or $1\nu_8$. However, the main problem of trying to fit the experimental results to theoretical ones is the lowest experimental wavenumber 704 cm^{-1}, for which there are no good matches in the calculated spectra. This leads to large differences between experimental and theoretical wavenumbers, up to 86 cm^{-1} at the MP2 method. Computed MAEs based on the smallest $\Delta\nu$ values for B3LYP and MP2 are 22 and 35 cm^{-1}, respectively. While this MAE is decent for DFT, it is very unlikely that MP2 would lead much higher MAE than for the minimum-energy HO conformer. Therefore, our anharmonic vibrational results indicate that the experimentally measured local minimum structure in an isolated argon matrix must be the HH conformer, as suggested already in a previous study by Lundell et al. [5].

It is notable that while the gas phase OO conformer has a lower activation energy to form from HO conformer rotation, and is also predicted to be lower in energy than the HH conformer, only the HH conformer has been isolated and measured (by IR spectroscopy) in an argon matrix. In the matrix isolation study by Lundell et al. [5], the energy applied to interconversion of conformers was as high as ca. 120 kcal/mol. Therefore, the identity of the obtained conformer can not be determined based on the height of the barrier of rotation.

Table 3
Experimental wavenumbers (ν in cm^{-1}) in Ar matrix, calculated anharmonic ν at B3LYP and MP2 methods for the HH conformer, differences between experimental and calculated wavenumbers ($\Delta\nu$), calculated anharmonic intensities (I in km/mol) for fundamentals (1ν), overtones (2ν) and highest intensity combination bands ($1\nu + 1\nu$), and assignment of vibrations for fundamental bands.

	Ar	B3LYP			MP2			assignment
	ν	ν	I	$\Delta\nu$	ν	I	$\Delta\nu$	
$1\nu_1$	2932	2881	53	51	2943	56	-11	H-Cstr., sym.
$1\nu_2$		2871	1		2919	1		H-Cstr., asym.
$1\nu_3$	1845	1867	34	-23	1831	16	14	O=Cstr., sym.
$1\nu_4$		1780	407		1753	550		O=Cstr., asym.
$1\nu_5$		1407	0		1415	1		CHrock, sym.
$1\nu_6$	1360	1355	6	5	1359	9	0	CHrock, asym.
$1\nu_7$		1101	97		1113	82		C-O-Cstr., sym.
$1\nu_8$	1039	1012	659	(27)	1033	705	6	C-O-Cstr., asym.
$1\nu_9$		1010	0		1006	0		CHwag., sym.
$1\nu_{10}$		1004	0		1003	0		CHwag., asym.
$1\nu_{11}$	704	702	56	2	698	45	6	O-C-Osciss., asym.
$1\nu_{12}$		523	0		526	0		O-C-Osciss., sym.
$1\nu_{13}$		272	9		276	12		C-O-Csciss.sym.
$1\nu_{14}$		169	0		179	0		O-Cwag., sym.
$1\nu_{15}$		128	4		125	5		C=Owag., sym.
$2\nu_1$		5662	0		5840	0		
$2\nu_2$		5514	1		5713	1		
$2\nu_3$		3724	0		3652	0		
$2\nu_4$		3574	1		3497	1		
$2\nu_5$		2778	19		2807	5		
$2\nu_6$		2699	1		2709	0		
$2\nu_7$		2196	0		2219	0		
$2\nu_8$		2018	0		2049	0		
$2\nu_9$		2009	0		2009	0		
$2\nu_{10}$		2005	0		2003	0		
$2\nu_{11}$		1402	0		1396	0		
$2\nu_{12}$	1039	1042	2	-3	1050	2	(-10)	
$2\nu_{13}$		544	0		551	0		
$\nu_{13} + \nu_4$		1811	256		1811	36		
$\nu_{11} + \nu_9$		2100	23		2132	23		
$\nu_7 + \nu_5$		3638	11		3565	13		
$\nu_{15} + \nu_4$		1139	2		1132	13		
$\nu_{14} + \nu_7$		1283	7		1307	7		

3.3. Raman spectra of formic acid anhydride

To the best of our knowledge there is no experimental Raman data for any of the FAA conformers. Olbert-Majkut et al. have measured Raman spectrum for a formic acid monomer and its dimer in an argon matrix [32]. They found that temperature of 19 K was optimal to obtain a good optical quality as matrix samples become too scattering for Raman measurements at lower temperatures and the formation of larger complexes is likely at higher temperatures. They used excitation laser with a wavelength of 532 nm in Raman measurements. As no measurements have been performed for FAA, we use same wavelength and temperature as in formic acid experiments to obtain theoretical Raman intensities.

We have computed Raman scattering activities for each conformer using B3LYP/aug-cc-pVTZ level of theory. Theoretical Raman intensities (I_i^R) are calculated from Raman scattering activities (S_i) for each harmonic wavenumber ν_i at an excitation energy of green light wavenumber $\nu_0 = 18797$ cm^{-1} (532 nm) at temperature $T = 19$ K [33] as

$$I_i^R = \frac{2\pi^2 h(\nu_0 - \nu_i)^4 S_i}{45c\nu_i(1 - \exp(-\frac{h\nu_i c}{k_B T}))}, \quad (1)$$

where c is the speed of light, h is the Planck constant and k_B is the Boltzmann constant. Harmonic wavenumbers, Raman scattering activities and Raman intensities are given in Table 5.

4. Conclusions

We have carried out anharmonic vibrational frequency calculations for formic acid anhydride to compare accurately measured and computational infrared spectra. As anharmonic calculations allow modeling of overtone and combination bands in addition of fundamentals, that expands the reliability of determining molecular conformers. Calculated anharmonic spectra involving fundamental, overtone and combination bands are extremely useful for analyzing different conformers, or even identify new chemical structures, from a high-resolution experimental IR spectra. In addition, Raman scattering activities (and theoretical Raman intensities) were calculated to supplement the understanding of molecular structures and to offer a computed data set for future experimental Raman studies.

While the MP2/aug-cc-pVTZ level yields highly accurate vibrational spectrum, it is computationally heavy and unfeasible for large molecules. Based on our benchmark calculations, density functionals B3LYP and B3LYP-D3 offer a good compromise between accuracy and computational cost. In combination with aug-cc-pVTZ basis set, B3LYP and B3LYP-D3 give good agreement with experiment, however, relatively small Pople's basis sets result even better agreement with experimental spectrum. The better performance of DFT with relatively small Pople's basis sets than large augmented triple zeta correlation consistent basis set can be attributed to the fact that Pople's basis sets are developed for DFT whereas correlation consistent basis sets are developed for *ab initio* methods. Using the 6-31+G(d) basis set with DFT

Table 4
Experimental wavenumbers (ν in cm^{-1}) in Ar matrix, calculated anharmonic ν at B3LYP and MP2 methods for OO conformer, and a difference between experimental and calculated wavenumbers ($\Delta\nu$) and calculated anharmonic intensities (I in km/mol) for fundamentals (1ν), overtones (2ν) and highest intensity combination bands ($1\nu + 1\nu$), and assignment of a vibration for fundamental bands.

	Ar	B3LYP			MP2			assignment
	ν	ν	I	$\Delta\nu$	ν	I	$\Delta\nu$	
$1\nu_1$	2932	2905	49	28	2973	27	(-41)	H-Cstr., sym.
$1\nu_2$	2932	2904	37	(28)	2968	36	-36	H-Cstr., asym.
$1\nu_3$	1845	1845	271	0	1809	215	(36)	O=Cstr., sym.
$1\nu_4$		1763	134		1728	147		O=Cstr., asym.
$1\nu_5$		1376	2		1380	1		C-Hrock, sym.
$1\nu_6$	1360	1360	1	-1	1366	4	-6	C-Hrock, asym.
$1\nu_7$	1039	1042	614	-3	1055	676	(-16)	C-O-Cstr.asym.
$1\nu_8$	1039	1025	0	(14)	1028	0	11	CHwag., asym.
$1\nu_9$		995	133		997	93		CHwag., sym.
$1\nu_{10}$		952	3		957	6		C-O-Cstr.,sym.
$1\nu_{11}$	704	781	30	-77	790	36	-86	O-C-Osciss., sym.
$1\nu_{12}$		555	10		546	10		O-C-Osciss., asym.
$1\nu_{13}$		209	1		183	19		C-O-Csciss.,sym.
$1\nu_{14}$		207	24		197	24		O-Cwag., sym.
$1\nu_{15}$		89	2		94	2		C=Owag., sym.
$2\nu_1$		5809	0		5826	1		
$2\nu_2$		5683	1		5946	0		
$2\nu_3$		3679	3		3607	4		
$2\nu_4$		3516	2		3448	3		
$2\nu_5$		2744	0		2753	0		
$2\nu_6$		2708	0		2721	0		
$2\nu_7$		2072	4		2097	3		
$2\nu_8$		2048	0		2053	0		
$2\nu_9$		1970	1		1975	0		
$2\nu_{10}$		1907	33		1914	8		
$2\nu_{11}$		1557	0		1574	0		
$2\nu_{12}$		1106	0		1089	0		
$2\nu_{13}$		412	0		365	0		
$2\nu_{14}$		404	0		384	0		
$2\nu_{15}$		160	0		202	9		
$\nu_{15}+\nu_6$		976	44		974	17		
$\nu_{13}+\nu_3$	1845	1816	25	(29)	1839	17	6	
$\nu_{15}+\nu_4$		1078	4		1085	11		
$\nu_{13}+\nu_7$		1728	3		1742	10		
$\nu_{13}+\nu_5$		1806	3		1818	8		

Table 5
Computed harmonic wavenumbers (ν in cm^{-1}), Raman scattering activities (S_i in $Å^4$/amu) and Raman intensities (I_i^R in m^2/sr) for HO, HH and OO conformers of FAA.

HO			HH			OO		
ν	S_i	I_i^R	ν	S_i	I_i^R	ν	S_i	I_i^R
3088	39.7	758	3011	128.8	2576	3048	185.0	3621
3057	137.9	2684	2989	0.5	9	3046	95.6	1873
1860	36.1	1549	1900	49.4	2057	1882	21.1	892
1809	5.7	254	1820	2.5	110	1795	6.0	270
1406	3.3	207	1440	3.5	211	1409	6.7	419
1380	4.7	302	1386	3.9	250	1393	0.7	45
1104	4.5	384	1131	2.1	179	1082	0.2	20
1046	1.8	168	1055	2.4	217	1045	2.2	198
1034	0.2	20	1028	1.4	135	1007	0.4	40
1004	3.3	317	1020	0.4	40	972	9.0	911
780	4.5	592	710	0.2	23	797	5.2	666
538	3.4	679	534	9.3	1869	562	3.1	594
252	1.7	782	274	0.6	267	216	1.1	569
224	0.9	489	178	0.4	283	210	1.9	1073
73	0.9	1398	131	0.1	59	103	2.5	2847

allows to extend anharmonic approach to the molecules of large size. Thus, we recommend to applying a suitable density functional with a small Pople's basis set in future vibrational spectroscopy studies of larger molecules.

Additionally, we studied potential energy surface of FAA. We found that B3LYP leads qualitatively wrong conformer energy order. Dispersion corrections are needed to predict that OO conformer is lower in energy than HH conformer. To yield quantitatively correct energy evaluation, single point energy corrections at a highly correlated electronic energy method, such as CCSD(T), are strongly recommended to employ on top of the DFT structures.

When analyzing the spectrum of the HO conformer of the FAA molecule, one frequency (exp. 1067 cm^{-1}) was reassigned. Instead of an asymmetric CH wagging with zero intensity ($1\nu_8$), it was assigned to an overtone $2\nu_{12}$ vibration with medium intensity. It is notable that a few intensities of combination bands are high, and could be visible in the spectrum. However, as their wavenumbers are close to those of high intensity fundamental peaks, they are difficult to identify as separate peaks. Additionally, one peak (exp. 1039 cm^{-1}) from the spectrum of the HH conformer was reassigned from a symmetric CH rocking with zero intensity ($1\nu_9$) to an asymmetric C-O stretching with strong intensity ($1\nu_8$). Also in this case, the highest intensity combination bands are difficult to identify due to a close-lying fundamental bands.

Formic acid anhydride has been shown to have a role in atmospheric Criegee chemistry and that reaction has been intensively studied with both experimental and theoretical tools [11–14,8]. Perhaps matrix-isolation vibrational spectroscopy can guide to study atmospheric reactions involving other reactive species such as peroxy and alkoxy radicals, which are under active investigation within atmospheric com-

munity, but surprisingly little is known experimentally about their exact structures and properties [34,35]. Additionally, understanding properties of small anhydride compounds may aid studies of larger multifunctional organic compounds which have direct relevance to aerosol particle formation and properties, and through it to Earth's radiative balance.

CRediT authorship contribution statement

Nanna Myllys: Writing – original draft, Methodology, Investigation, Funding acquisition, Formal analysis, Data curation, Conceptualization. **Irina Osadchuk:** Investigation, Data curation. **Jan Lundell:** Writing – review & editing, Supervision, Funding acquisition.

Declaration of competing interest

The authors declare that they have no known competing financial interests or personal relationships that could have appeared to influence the work reported in this paper.

Data availability

Data will be made available on request.

Acknowledgements

We thank the Academy of Finland for funding (grants no. 332023 and 347775) and the CSC-IT Center for Science in Espoo, Finland, for computational resources. We thank Dr. Luis Duarte and Prof. Theo Kurtén for fruitful comments.

Appendix A. Supplementary material

Supplementary material related to this article can be found online at https://doi.org/10.1016/j.molstruc.2024.137643.

References

[1] H. Kühne, T.-K. Ha, R. Meyer, H.H. Günthard, Formic acid anhydride: matrix infrared spectra of five isotopic species, vibrational analysis, empirical and ab initio harmonic force field and thermodynamic functions, J. Mol. Spectrosc. 77 (2) (1979) 251–269.
[2] E.A. Noe, M. Raban, Dynamic nuclear magnetic resonance investigation of formic anhydride. Conformation and torsional barrier, J. Chem. Soc., Chem. Commun. 12 (1974) 479–480.
[3] I.G. John, L. Radom, Molecular conformations of formic anhydride and divinyl ether an ab initio molecular orbital study, J. Mol. Struct. 39 (2) (1977) 281–293.
[4] S. Vaccani, U. Roos, A. Bauder, H.H. Günthard, Microwave spectra, substitution structure and vibrational satellites of formic anhydride, Chem. Phys. 19 (1) (1977) 51–57.
[5] J. Lundell, M. Räsänen, T. Raaska, J. Nieminen, J. Murto, Matrix isolation infrared and ab initio studies on conformers of formic acid anhydride, J. Phys. Chem. 97 (18) (1993) 4577–4581.
[6] J. Lundell, M. Räsänen, Matrix-isolated binary and ternary complexes formed in photochemical decomposition of formic acid anhydride, J. Phys. Chem. 97 (38) (1993) 9657–9663.
[7] G. Wu, S. Shlykov, F. Van Alseny, H. Geise, E. Sluyts, B. Van der Veken, Formic anhydride in the gas phase, studied by electron diffraction and microwave and infrared spectroscopy, supplemented with ab-initio calculations of geometries and force fields, J. Phys. Chem. 99 (21) (1995) 8589–8598.
[8] C.-A. Chung, J.W. Su, Y.-P. Lee, Detailed mechanism and kinetics of the reaction of criegee intermediate ch 2 oo with hcooh investigated via infrared identification of conformers of hydroperoxymethyl formate and formic acid anhydride, Phys. Chem. Chem. Phys. 21 (38) (2019) 21445–21455.
[9] D.A. Good, J.S. Francisco, Tropospheric oxidation mechanism of dimethyl ether and methyl formate, J. Phys. Chem. A 104 (6) (2000) 1171–1185.
[10] O. Welz, A.J. Eskola, L. Sheps, B. Rotavera, J.D. Savee, A.M. Scheer, D.L. Osborn, D. Lowe, A. Murray Booth, P. Xiao, et al., Rate coefficients of C1 and C2 criegee intermediate reactions with formic and acetic acid near the collision limit: direct kinetics measurements and atmospheric implications, Angew. Chem., Int. Ed. 53 (18) (2014) 4547–4550.
[11] D.L. Osborn, Reaction mechanisms on multiwell potential energy surfaces in combustion (and atmospheric) chemistry, Annu. Rev. Phys. Chem. 68 (2017) 233–260.
[12] B. Long, J.-R. Cheng, X.-f. Tan, W.-j. Zhang, Theoretical study on the detailed reaction mechanisms of carbonyl oxide with formic acid, J. Mol. Struct., Theochem 916 (1–3) (2009) 159–167.
[13] A. Andersen, E.A. Carter, Hybrid density functional theory predictions of low-temperature dimethyl ether combustion pathways. II. Chain-branching energetics and possible role of the criegee intermediate, J. Phys. Chem. A 107 (44) (2003) 9463–9478.
[14] C. Cabezas, Y. Endo, The criegee intermediate-formic acid reaction explored by rotational spectroscopy, Phys. Chem. Chem. Phys. 21 (33) (2019) 18059–18064.
[15] A. Boogaard, H. Geise, F. Mijlhoff, An electron diffraction investigation of the molecular structure of formic anhydride, J. Mol. Struct. 13 (1) (1972) 53–58.
[16] S. Vaccani, A. Bauder, H.H. Günthard, Microwave spectrum, dipole moment and conformation of formic anhydride, Chem. Phys. Lett. 35 (4) (1975) 457–460.
[17] P. Aplincourt, M. Ruiz-López, Theoretical study of formic acid anhydride formation from carbonyl oxide in the atmosphere, J. Phys. Chem. A 104 (2) (2000) 380–388.
[18] M. Head-Gordon, J.A. Pople, M.J. Frisch, Mp2 energy evaluation by direct methods, Chem. Phys. Lett. 153 (6) (1988) 503–506.
[19] R.A. Kendall, T.H. Dunning Jr., R.J. Harrison, Electron affinities of the first-row atoms revisited. Systematic basis sets and wave functions, J. Chem. Phys. 96 (9) (1992) 6796–6806.
[20] A.D. Becke, Density-functional thermochemistry. III. The role of exact exchange, J. Chem. Phys. 98 (7) (1993) 5648–5652, https://doi.org/10.1063/1.464913, http://link.aip.org/link/?JCP/98/5648/1.
[21] A.D. Becke, A new mixing of Hartree–Fock and local density-functional theories, J. Chem. Phys. 98 (2) (1993) 1372–1377, https://doi.org/10.1063/1.464304, http://link.aip.org/link/?JCP/98/1372/1.
[22] C. Lee, W. Yang, R.G. Parr, Development of the colle-salvetti correlation-energy formula into a functional of the electron density, Phys. Rev. B 37 (2) (1988) 785.
[23] S. Grimme, J. Antony, S. Ehrlich, H. Krieg, A consistent and accurate ab initio parametrization of density functional dispersion correction (dft-d) for the 94 elements h-pu, J. Chem. Phys. 132 (15) (2010) 154104.
[24] V. Barone, Anharmonic vibrational properties by a fully automated second-order perturbative approach, J. Chem. Phys. 122 (1) (2005) 014108.
[25] V. Barone, J. Bloino, C.A. Guido, F. Lipparini, A fully automated implementation of vpt2 infrared intensities, Chem. Phys. Lett. 496 (1–3) (2010) 157–161.
[26] M.J. Frisch, G.W. Trucks, H.B. Schlegel, G.E. Scuseria, M.A. Robb, J.R. Cheeseman, G. Scalmani, V. Barone, G.A. Petersson, H. Nakatsuji, X. Li, M. Caricato, A.V. Marenich, J. Bloino, B.G. Janesko, R. Gomperts, B. Mennucci, H.P. Hratchian, J.V. Ortiz, A.F. Izmaylov, J.L. Sonnenberg, D. Williams-Young, F. Ding, F. Lipparini, F. Egidi, J. Goings, B. Peng, A. Petrone, T. Henderson, D. Ranasinghe, V.G. Zakrzewski, J. Gao, N. Rega, G. Zheng, W. Liang, M. Hada, M. Ehara, K. Toyota, R. Fukuda, J. Hasegawa, M. Ishida, T. Nakajima, Y. Honda, O. Kitao, H. Nakai, T. Vreven, K. Throssell, J.A. Montgomery Jr., J.E. Peralta, F. Ogliaro, M.J. Bearpark, J.J. Heyd, E.N. Brothers, K.N. Kudin, V.N. Staroverov, T.A. Keith, R. Kobayashi, J. Normand, K. Raghavachari, A.P. Rendell, J.C. Burant, S.S. Iyengar, J. Tomasi, M. Cossi, J.M. Millam, M. Klene, C. Adamo, R. Cammi, J.W. Ochterski, R.L. Martin, K. Morokuma, O. Farkas, J.B. Foresman, D.J. Fox, Gaussian16 Revision A.03, 2016.
[27] F. Neese, The ORCA program system, Wiley Interdiscip. Rev. Comput. Mol. Sci. 2 (1) (2012) 73–78, https://doi.org/10.1002/wcms.81.
[28] F. Neese, Software update: the ORCA program system, version 4.0, Wiley Interdiscip. Rev. Comput. Mol. Sci. 8 (1) (2018) e1327.
[29] L. Kong, F.A. Bischoff, E.F. Valeev, Explicitly correlated R12/F12 methods for electronic structure, Chem. Rev. 112 (1) (2012) 75–107.
[30] N. Chéron, D. Jacquemin, P. Fleurat-Lessard, A qualitative failure of b3lyp for textbook organic reactions, Phys. Chem. Chem. Phys. 14 (19) (2012) 7170–7175.
[31] H. Kruse, L. Goerigk, S. Grimme, Why the standard b3lyp/6-31g* model chemistry should not be used in dft calculations of molecular thermochemistry: understanding and correcting the problem, J. Org. Chem. 77 (23) (2012) 10824–10834.
[32] A. Olbert-Majkut, J. Ahokas, J. Lundell, M. Pettersson, Raman spectroscopy of formic acid and its dimers isolated in low temperature argon matrices, Chem. Phys. Lett. 468 (4–6) (2009) 176–183.
[33] D.A. Long, The Raman Effect: a Unified Treatment of the Theory of Raman Scattering by Molecules, Wiley, 2002.
[34] M. Ehn, T. Berndt, J. Wildt, T. Mentel, Highly oxygenated molecules from atmospheric autoxidation of hydrocarbons: a prominent challenge for chemical kinetics studies, Int. J. Chem. Kinet. 49 (11) (2017) 821–831.
[35] F. Bianchi, T. Kurtén, M. Riva, C. Mohr, M.P. Rissanen, P. Roldin, T. Berndt, J.D. Crounse, P.O. Wennberg, T.F. Mentel, et al., Highly oxygenated organic molecules (hom) from gas-phase autoxidation involving peroxy radicals: a key contributor to atmospheric aerosol, Chem. Rev. 119 (6) (2019) 3472–3509.